Effect of Marine Growth on Floating Wind Turbines Mooring Lines Responses

C. SPRAUL[a], H-D. PHAM[b], V. ARNAL and M. REYNAUD

a. Laboratoire de recherche en Hydrodynamique, Énergétique et Environnement Atmosphérique - *UMR CNRS 6598*, Nantes, France *charles.spraul@ec-nantes.fr*
b. Institut de Recherches en Génie Civil et Mécanique - *UMR CNRS 6183*, Nantes, France *hong-duc.pham@ec-nantes.fr*

Abstract:

Currently, pilot farms of floating wind turbines (FWT) are to be installed in depths between 50m and 100m. At these depths a large part of mooring lines and power cable length is susceptible to be covered with marine growth thus affecting the mass and hydrodynamic properties of these slender structures. Offshore standards published recommendations on the data required for taking into account the bio-colonization of the lines. However marine growth characteristics are largely site dependent, time dependent (seasonal variability) and also depend on the support surface, thus inducing a great variability in the quantities of biomass present on the lines. Furthermore, marine growth distribution along the lines length is generally assumed to be uniform, while in some cases large amounts of marine growth might be concentrated over small portions of the lines. The purpose of this work is to assess the impact of the quantity of marine growth on the dynamic behavior of mooring lines of floating wind turbines in a shallow water site, as well as the effect of its distribution.
Measurements at SEM-REV test site were made in order to quantify the development of local marine species on mooring lines. Identification of the species on site allows assumptions to be made on their repartition and growth rate. These assumptions are checked against on-site observations which quantify the thickness variations with depth. Marine growth parameters are then transposed in terms of line mass and hydrodynamic properties to be used in numerical simulations.
A numerical test case configuration is defined, inspired by the FLOATGEN European project's FWT to be installed at SEM-REV test site. The dynamic responses of the mooring lines are computed for this configuration using time domain numerical simulations. A modal analysis is conducted in order to observe the evolution of the natural frequencies of the mooring lines when subjected to different scenarios of bio-colonization. Influence of the bio-colonization is then assessed for real sea states.

Key Words: Floating Wind Turbines, Shallow water, Marine Growth, Taut Synthetic Moorings

1 Introduction

The impact of the marine growth on renewable energy structures such as FWT and wave energy converters (WEC) can be significant and has to be accounted for in the design phases. It however largely depends on the considered sites, devices and selected mooring systems.
Yang et al. [3] have evaluated the impact of marine growth on chain catenary mooring

lines for a WEC, and found an average decrease of 20 % in the fatigue life of the mooring lines due to the bio-colonization.
A recent study of Wright et al. [4] also showed a negative effect of marine growth presence on the platform of a tension moored floating wind turbine as the tendon tension was considerably decreased. That study was conducted on vertical taut mooring lines (TLP), for which slack tendon could induce great damage. The system analyzed here is different as it employs a softer mooring system with near horizontal taut mooring lines.

The mooring configuration studied in this paper is derived from the 2 MW floating wind turbine (FWT) which is to be installed on the SEM-REV test site in 2017 as part of the FP7-EU FLOATGEN project. The French Atlantic test site SEM-REV [1] [2] is located 20 km off the coast of le Croisic in Loire Atlantique. The mean water depth on site is taken at 36 m in this study.
However, the floater and moorings characteristics used in the study were selected only for this study purpose and are not representative of the FLOATGEN real mooring system. The considered FWT has a mass of about 5000 t and a draft of about 7 m. The floater, derived from those developed by IDEOL, is considered in this study as a square ring with a 36 m width, a height of 10 m, and a 21 m wide moonpool. The wind turbine's nacelle is located 60 m above the free surface.

This study focuses on the dynamic behavior of the mooring lines when subjected to different scenarios of marine growth. As a consequence, instead of the Chain-Nylon-Chain mooring line which is intended to be installed in order to prevent seabed friction and friction/compression around the fairlead, the simplified mooring system is composed of Nylon lines only. Thus, the results in part 4 and 5 should be considered for a very simplified mooring system which is not capturing the full dynamic behavior of the final mooring system on the SEM-REV site.

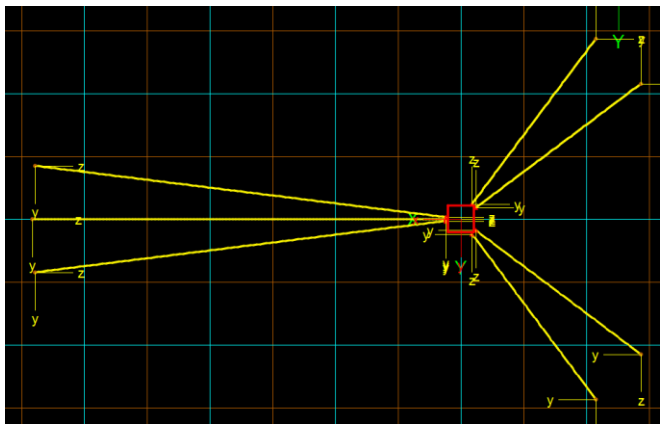

Figure 1.1: Top view of the simplified mooring layout used for the study

Figure 1.1 presents a top view of the FWT system with its mooring system. 7 mooring lines are considered in the analysis in order to ensure a static balance between front and rear lines with the selected positioning.
In part 2, comparisons are made between bio fouling measurements on the SEM-REV site, on submerged lines, and norms recommendations. Then the marine growth properties considered in the study are defined based on those observations. In part 3, details about the mechanical and hydrodynamic properties of the mooring lines and

how they are affected by the marine growth are introduced. Then in part 4 an analysis is conducted on a single mooring line in harmonic excitation to observe the effect of marine growth on natural frequencies. An attempt to extrapolate the marine growth influence to a full mooring system is led in part 5 in which we consider irregular sea states.

2 Marine Growth Characterization

Bio colonization affects immerged structures in several ways. For instance, it increases the mass, the volume and the hydrodynamic loads through diameter increase, but also by affecting the vortices formation mechanisms. Standards have thus published recommended practices to account for the marine growth in the design of immerged structures if a regular cleaning is not planned. Values in the following table are provided for use in Atlantic North or in the North Sea when more accurate data are unavailable. Down to 40 m depth, a constant thickness with constant density and roughness can be used. Marine growth thickness is assumed to increase at a constant rate during the first two years following installation, from 0 mm to 100 mm, and then to remain stable.

Table 2.1: Recommended Practice for marine growth [5][6][7]

Depth (m)	Thickness (mm)	Roughness (mm)	Density (kg/m^3)
+2	100	20	1330
-40			
Below -40	50		

However the bio colonization process is more complex and depends heavily on the considered site and it is usually recommended to characterize it through on-site. Even for North Sea offshore sites, measurements conducted on platforms during decommissioning revealed different repartition and weight of the marine growth than the values recommended by the standards [8]. Macleod et al. [9] highlighted the uncertainties and requirements for accurately measuring bio-colonization parameters, and insisted on the site-dependence.

Acquisition of data on SEM-REV test site:

Environmental monitoring is ongoing at the SEM-REV site structures since 2009. During maintenance operations of the floaters deployed at SEM-REV (weather buoys, special marking…), pictures and videos are systematically taken (figure 2.1). These images allowed the identification of the species colonizing the mooring lines. Dominant species were found to be algae (laminaria, fucales and ulva), hydrozoans and mussels (mytilus edulis). Considering their mass and their quantity, the mussels which are observed through the whole water column seem to be the driving specie for the purpose of design. In addition, three videos taken by the divers during maintenances were further analyzed to determine the thickness of the mussels' colonies as a function of depth. These data were obtained for 3.4 cm diameter synthetic mooring lines that had been immerged for 17 to 19 months. The data are presented on figure 2.2.

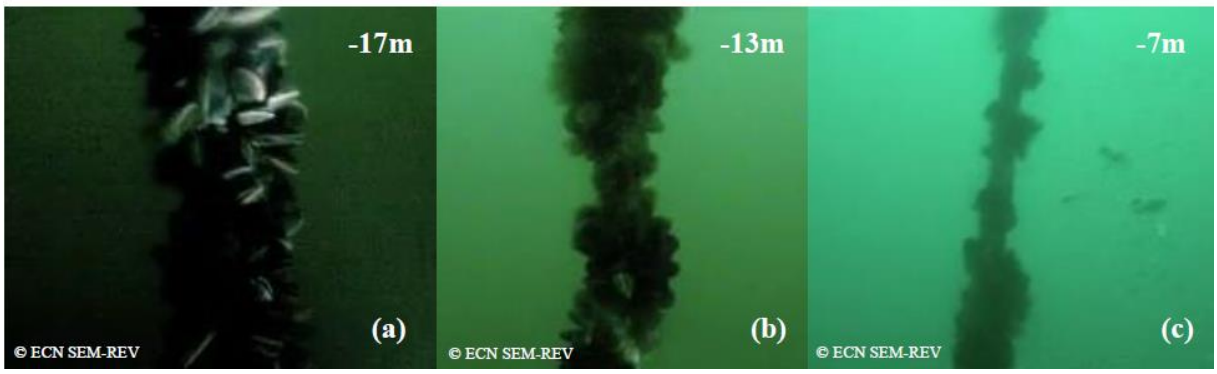

Figure 2.1: Illustration of Mytilus edulis colonization at SEMREV sea test site

During one of the operations, a mussel colony was sampled and weighted. As a result:

- 178 specimens were sampled from a 20 cm mooring line section
- The total weight measured was 2.6 kg (12.9 kg per meter)
- The mussel layer was 7.3 cm thick (line diameter: 3.4 cm)

Thus the marine growth layer volume was 0.021 m^3/m. Assuming that the mussels occupy between 10% and 40% of that volume and the rest is water, the layer density is found to be between 1100 kg/m^3 and 1400 kg/m^3. However as the actual fraction of volume occupied by the mussels is unknown this is only a rough estimation and the density value given in the norms will be used instead.

In subsequent sections, the considered mooring lines have a diameter of 19 cm and thus offer much more surface for marine species to settle on. However it is assumed that the same thickness and same density can be used for the marine growth layer.

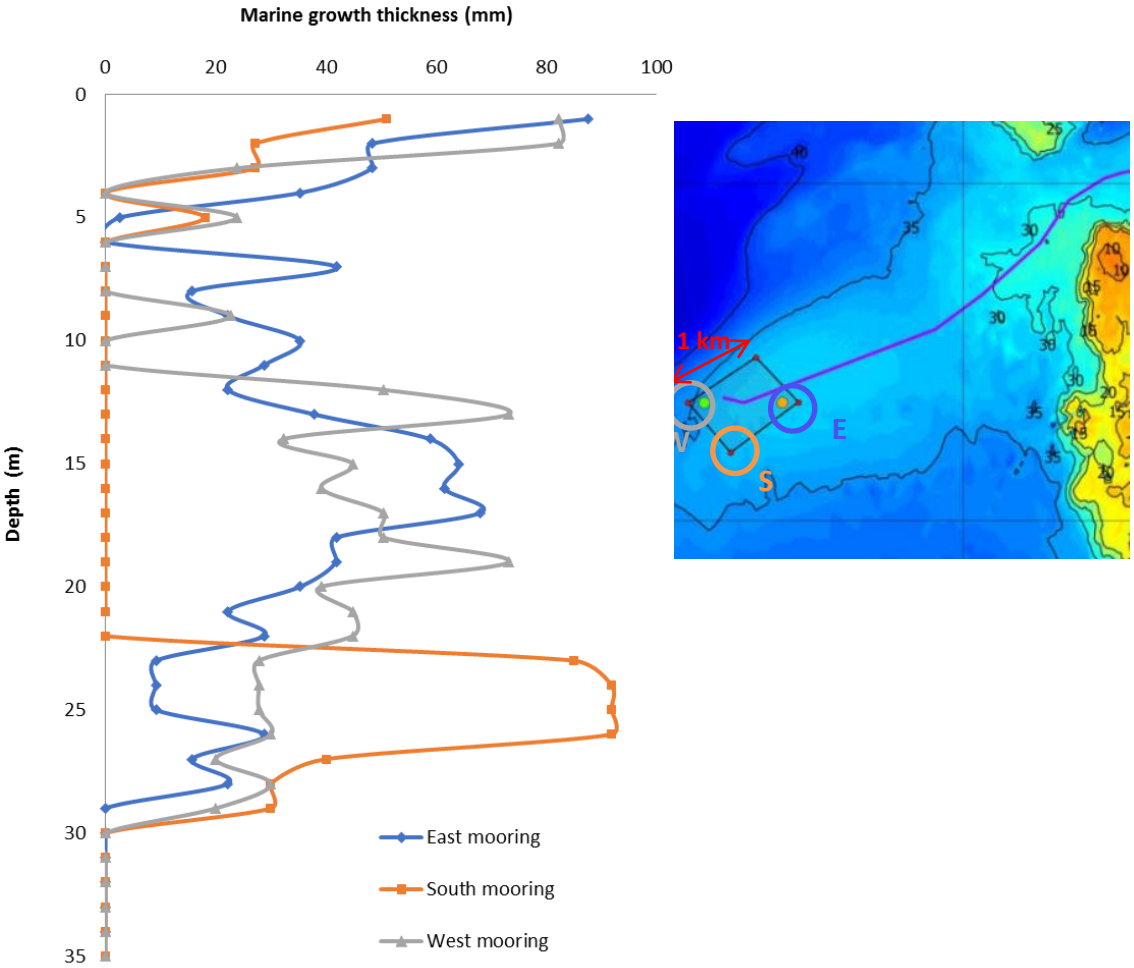

Figure 2.2: Marine growth thickness measurements

3 Mooring Lines Properties

Nomenclature:

e	Marine growth thickness	ρ	Water density
D_0	Bare line diameter	ρ_{mg}	Marine growth density
M_0	Bare line mass	$\vec{a}$	Line acceleration
D	Line diameter	$\overrightarrow{a_f}$	Fluid acceleration
V	Line volume (per unit length)	$\vec{v}$	Line velocity
M	Line mass (per unit length)	$\overrightarrow{v_f}$	Fluid velocity
M_a	Line added mass	C_d	Drag coefficient
L	Line length	C_a	Added mass coefficient
T	Line tension		

3.1 Without Marine Growth

The Nylon line considered in this study has a diameter of 19 cm. At the pretension of 20% of the MBL (Minimum breaking load), an axial stiffness of 52 MN can be considered a correct approximation of the line axial behavior. Torsional behavior is not considered here and the bending stiffness is set to zero.

The mass of the line is 31 kg/m while its volume is 0.028 m³/m. Thus including buoyancy the net under water weight of the line is 2.3 kg/m.

In the numerical simulations presented below, the hydrodynamic loads on the line are computed using Morison's equation [10]. The drag coefficient Cd value is set to 1.2 and the added mass coefficient Ca to 1.05. This value of drag coefficient is not representative of the whole range of Reynolds and Keulegan Carpenter numbers studied here. Furthermore, the drag coefficient should also be influenced by the higher roughness due to marine growth presence [11][12]. However, for the sake of simplicity and comparison, the same value is applied for all cases.

$$\overrightarrow{F_{Hd}} = \rho V \, \overrightarrow{a_f} + \rho V C_a \left(\overrightarrow{a_f} - \vec{a}\right) + \frac{1}{2}\rho D C_d \left\|\overrightarrow{v_f} - \vec{v}\right\| \left(\overrightarrow{v_f} - \vec{v}\right)$$

Table 3.1: Mooring lines properties

Diameter	EA	Mass	Volume	Drag Coefficient	Added Mass Coefficient
0.19 m	52 MN	31 kg/m	0.028 m³/m	1.2	1.05

3.2 With Marine Growth

In this study the marine growth on the line is modelled as a homogenous layer around the line, with fixed thickness and density properties. This implies that the density value also accounts for the water volume trapped inside the marine growth layer.
It is considered that the marine growth does not modify the structural properties of the line, such as its axial and bending stiffness. Drag and added mass coefficients are also kept the same, therefore only the mass and diameter are affected.
The modification of diameter although affects the buoyancy, drag force and added mass of the cable.

Table 3.2: Effect of the marine growth layer's thickness on mooring lines properties

Layer Thickness	Layer Density	Diameter	Volume	Mass	Drag	Added Mass
0 cm	1330 kg/m³	0.19 m	0.028 m³/m	31 kg/m	117 N/(m/s)²/m	31 kg/m
8 cm	1330 kg/m³	0.35 m	0.096 m³/m	121 kg/m	215 N/(m/s)²/m	104 kg/m

$$D = D_0 + 2\,e$$
$$V = \frac{\pi}{4}\,D^2$$
$$M = M_0 + \frac{\pi}{4}\,(D^2 - D_0^2)\,\rho_{mg}$$
$$Drag = \frac{1}{2}\,\rho D\,C_d$$
$$M_a = \rho V\,C_a$$

3.3 Marine Growth distribution

In order to account for the non-uniform distribution of the marine growth along the cable length, different thickness values are applied depending on water depth (see figure 3.1 for illustration).
In the numerical model mass, volume, drag and added mass properties are all lumped to the nodes. Therefore a thickness value is attributed to each node depending on its depth. Other marine growth properties (mass, volume and added drag area) are then computed

based on the thickness value and the fixed density value, and are all applied directly to the node.
In the numerical model the line is discretized into 5m long segments. As the lines are close to horizontal this give a vertical discretization below 0.5m.

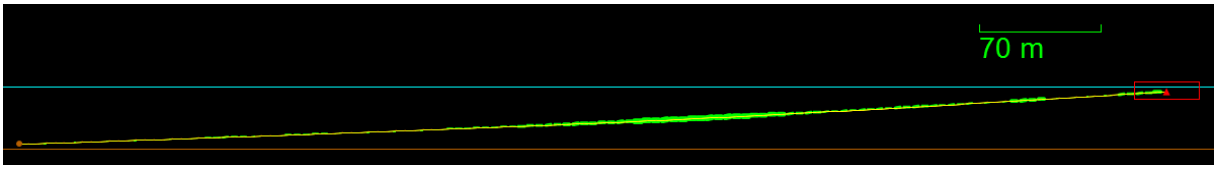

Figure 3.1: OrcaFlex model accounting for marine growth distribution

4 Marine Growth Effect on Line's Natural Frequencies

The natural frequencies of the taut mooring lines can be estimated using the string vibration theory [10] for out-of-line vibrations:

$$f_n = \frac{n}{2\,L}\sqrt{\frac{T}{M + M_a}}$$

The pre-tension value is set identical for all the lines to a value of 2 MN (20% of the minimum breaking load). The front lines length is 660m (figure 4.1), while rear lines are only 330m long (figure 4.2). The effective mass and added mass of the line depend on the test case.

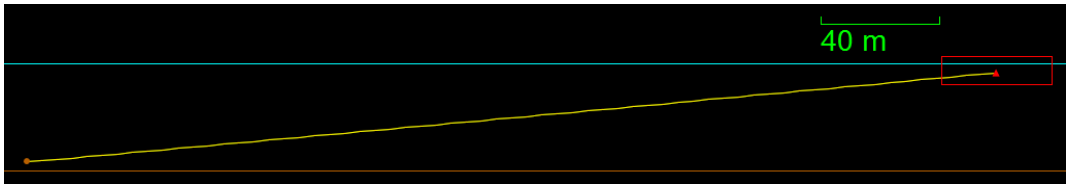

Figure 4.1: Rear line view in OrcaFlex

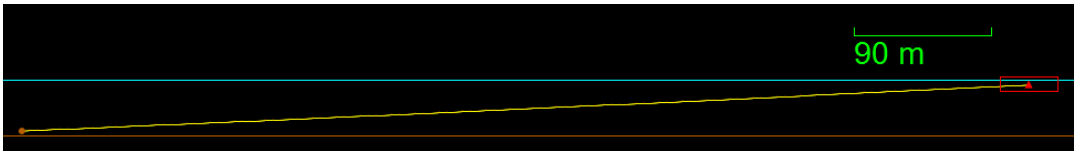

Figure 4.2: Front line view in OrcaFlex

7 test cases are studied with different marine growth quantity or distribution.

- Case 0 is the reference considering no marine growth on the line.
- Case 1 considers a uniform marine growth distribution with a thickness of 8 cm which is about the maximum observed on the line during the measurements and close to the standard recommendations.
- Cases 2 and 3 also consider a uniform distribution, marine growth thickness is set however to match the total mass observed respectively for the South buoy measurements and for the East and West buoys measurements.
- Cases 2.1, 3.1 and 3.2 on the other hand consider the observed distributions, respectively for buoys South, East and West.

The first natural frequency of both front and rear lines were computed for cases 0, 1, 2 and 3, and are given in table 4.2 and 4.3. As the line mass increases with the quantity of marine growth the natural frequencies are shifted toward larger periods, and especially

towards periods at which the FWT floater is susceptible to experience larger motions in response to the waves.

Table 4.1: Cases presentation

	Case 0	Case 1	Case 2	Case 3	Case 2.1	Case 3.1	Case 3.2
Equivalent average thickness	0 cm	8 cm	2.04 cm	2.77 cm	2.04 cm	2.77 cm	2.77 cm
Distribution	uniform	uniform	uniform	uniform	non uniform	non uniform	non uniform

Table 4.2: First natural frequency of rear lines (330m):

	Case 0	Case 1	Case 2	Case 3
Frequency	0.273 Hz	0.143 Hz	0.221 Hz	0.207 Hz
Period	3.7 s	7.0 s	4.5 s	4.8 s

Table 4.3: First natural frequency of front lines (660m):

	Case 0	Case 1	Case 2	Case 3
Frequency	0.137 Hz	0.072 Hz	0.111 Hz	0.104 Hz
Period	7.3 s	14.0 s	9.0 s	9.7 s

In order to assess the magnitude of the response to those natural frequencies, time domain dynamic simulations are run using OrcaFlex [7] for a range of excitation frequencies.
Three directions of excitation are studied. As the considered natural frequencies concern out-of-line vibrations, horizontal and (near) vertical harmonic excitations are applied at the fairlead in the plane orthogonal the line axis. Though natural frequencies for the in-line response are far above wave frequencies, in-line excitation are also applied as the expected quasi static response amplitude is much larger.
The amplitude of the excitation is set to 0.5 m for all the frequencies; however 1 m amplitude was also tested to assess the effect of larger amplitudes. For high frequencies the 0.5 m amplitude is too large to be representative of the floater motion, but other sources of excitation can act at these frequencies, like vortex induced vibrations. On the other hand, for low frequencies larger motion can be expected.

Comparison is made considering the tension amplitude at the fairlead. To highlight the dynamic effects the DAF (dynamic amplification factors), ratio between dynamic response and quasi static response, are also compared.

4.1 Effect of Marine Growth quantity

To quantify the effect of the quantity of marine growth on the dynamic response of the cable, comparison is made between cases 0, 1 and 2. For all these cases the distribution is uniform and only the marine growth thickness varies.

Table 4.4: Response at the largest peak period (out-of-line):

		Rear line (330 m)			Front line (660 m)		
		0 cm	2.04 cm	8 cm	0 cm	2.04 cm	8 cm
Vertical 0.5 m	Period	3.3 s	4.2 s	6.7 s	6.7 s	8.3 s	12.5 s
	DAF	9.8	22	96	26	85	372
Vertical	Period	3.6 s	4.3 s	6.7 s	6.7 s	8.3 s	12.5 s

1.0 m	DAF	5.2	9.8	37	11	34	144
Vertical	Period	-	5.0 s	7.1 s	7.7 s	9.1 s	14.3 s
3.0 m	DAF	-	4.0	9.2	5.4	9.3	36

Considering out-of-line excitation, it is observed that amplitudes are larger with vertical excitation than with horizontal excitation which is due to the work of the weight force. Also the dynamic amplification factor decreases as the excitation amplitude increases.
The dynamic amplification factors are much larger in the case with 8 cm marine growth than in the case without marine growth. With 2.04 cm of marine growth a significant amplification is observed, much less however than with 8 cm.
However, even with 8 cm marine growth, tension amplitudes remain very low when compared to the 2 MN pre-tension.

Considering in-line excitation, the natural frequencies are also made lower with the addition of marine growth. Those natural frequencies however remain far above the frequency range at which the floater responds. On the other hand a significant reduction of amplitude is observed at the fairlead at twice the first in-line natural frequency of the line. Considering the fairlead as a vibration antinode, this is indeed the first natural frequency of a line twice as long.
Even though this amplitude trough is located at a period at which the floater is unlikely to have a large response, the amplitude reduction is still quite large at a 10 s period for the front line with 8 cm marine growth.
This amplitude trough is not observed at the anchor (Figure 4.6) where on the contrary the addition of marine growth tend to increase the tension amplitude.

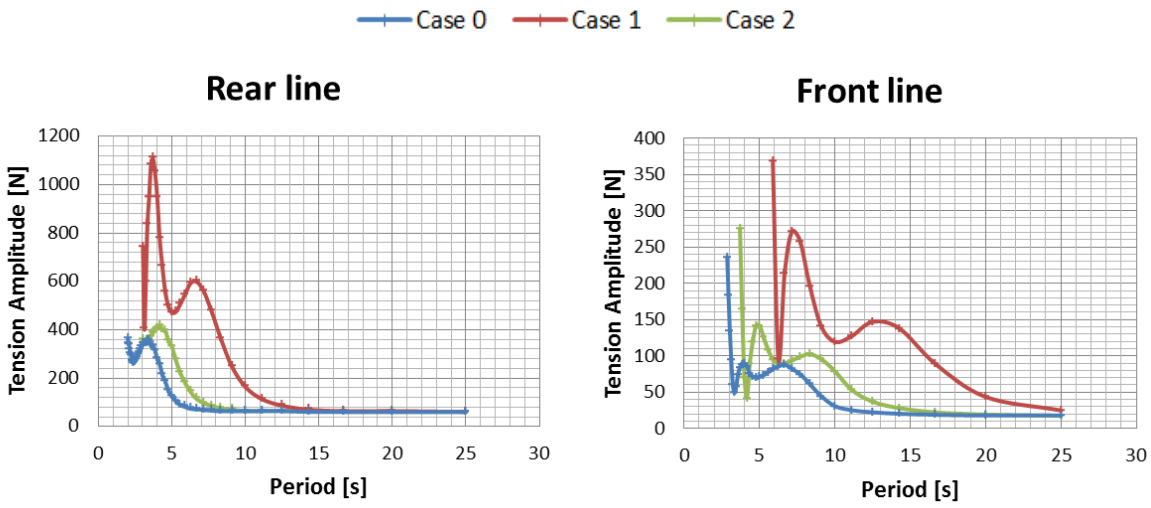

Figure 4.3: Line response at fairlead to horizontal excitation (0.5m) for different marine growth thicknesses

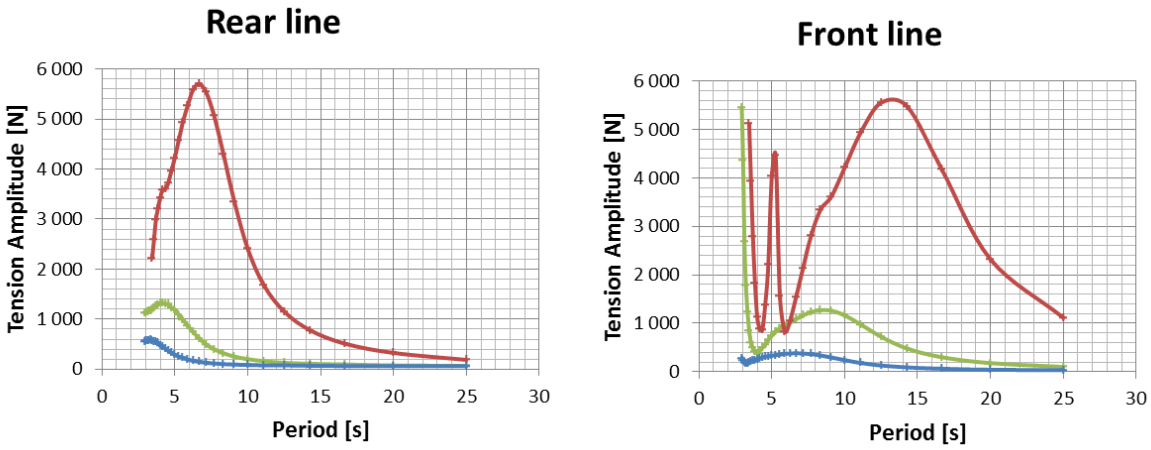

Figure 4.4: Line response at fairlead to vertical excitation (0.5m) for different marine growth thicknesses

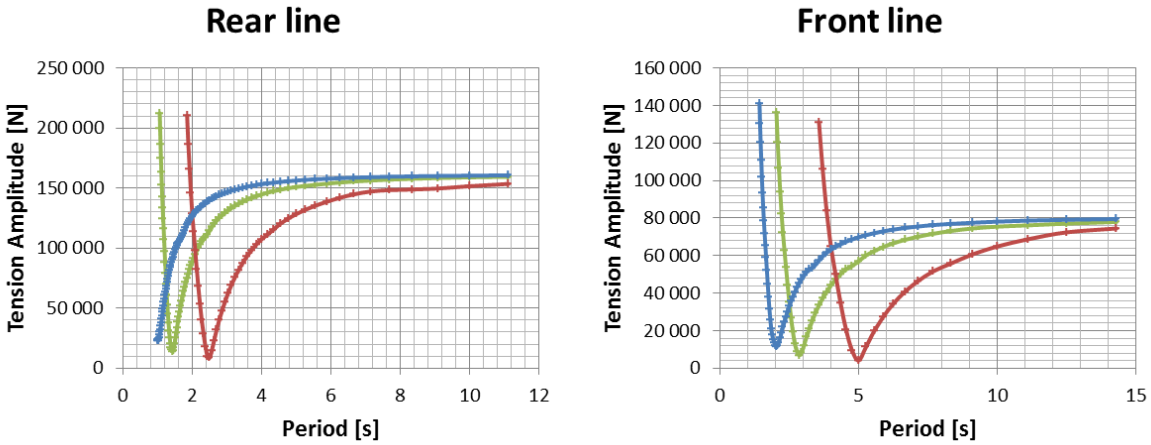

Figure 4.5: Line response at fairlead to in-line excitation (0.5m) for different marine growth thicknesses

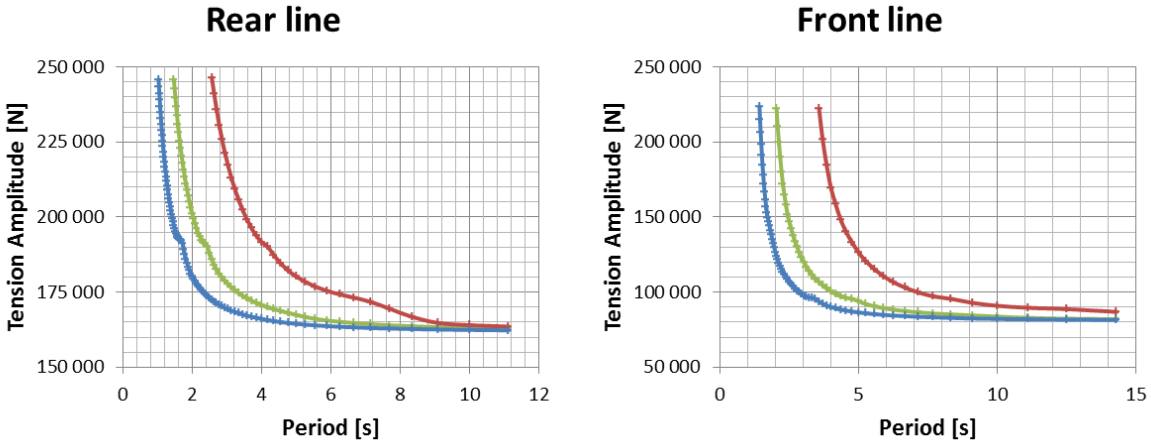

Figure 4.6: Line response at anchor to in-line excitation (0.5m) for different marine growth thicknesses

4.2 Effect of Marine Growth distribution

To observe the effect of marine growth distribution, the cases 2.1, 3.1 and 3.2 which distributions are non-uniform, and which are respectively corresponding to South, East and West buoy measurements, are compared to cases 2 and 3 which respectively consider the same total mass of marine growth.
Comparison is made for in-line excitation with amplitude 0.5 m. On the figures below, the response of the lines without marine growth are also plotted to serve as references.

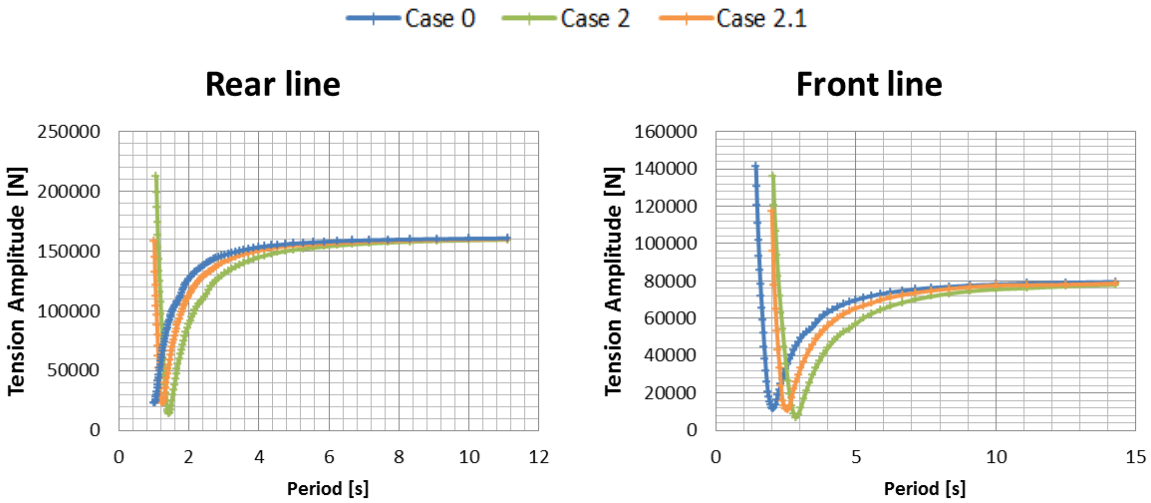

Figure 4.7: Line response at fairlead to in-line excitation (0.5m) for different marine growth distributions (South buoys)

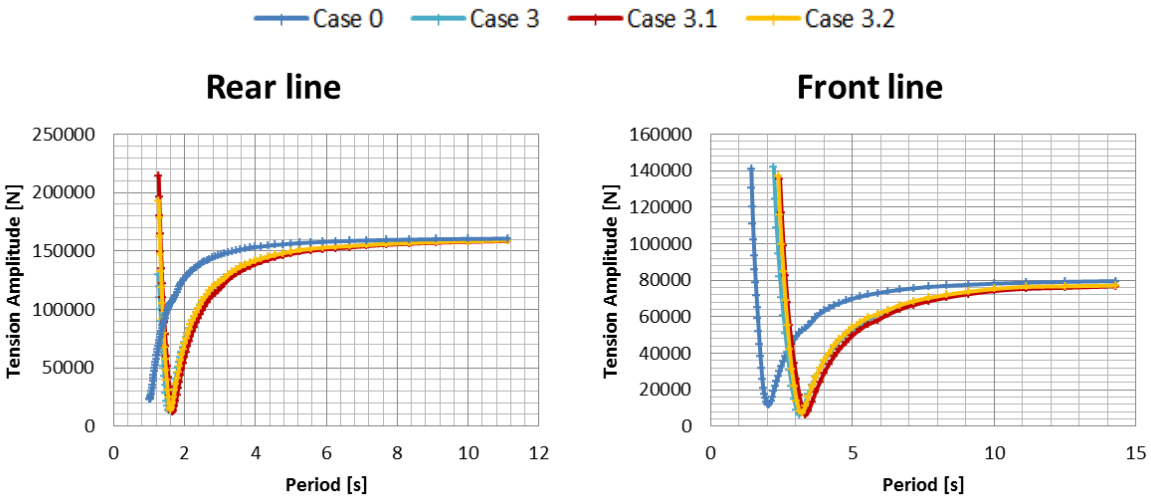

Figure 4.8: Line response at fairlead to in-line excitation (0.5m) for different marine growth distributions (East and West buoys)

The distribution of the marine growth along the line appears to have some effect between cases 2 and 2.1 for periods around the trough. On the other hand for cases 3.1 and 3.2, the line response is nearly the same as for case 3. A possible explanation is that for case 2.1 nearly all the mass is concentrated over a small area whereas for cases 3.1 and 3.2 the mass is more distributed.

Though amplitudes at fairlead and anchor do not seem to be much affected by the marine growth distribution, the distribution of tension along the line is modified.
For out-of-line excitation, larger differences are observed. Depending on the natural mode that is excited, the peak amplitude and frequency can be either increased or decreased. In all case though, the effect of the distribution appears to be less important than that of the total mass of marine growth.

5. Application to coupled mooring analysis in severe sea states

5.1 Load cases

The sea conditions studied are chosen from SEM-REV observation [14] regarding to two sea conditions of concern in the design of mooring lines (extreme state and fatigue state), table 5.1.

Table 5.1: Sea states used in the calculation

Sea state	Spectrum type	Hs (m)	Tp(s)	Gamma
1	JONSWAP	10	15	3.3
2	JONSWAP	1	10	3.3

5.2 Application

The objective of this section is to assess the impact of marine growth on the dynamic behaviors of the mooring lines in real sea conditions. For simplification, the wind load, current load and the second order drift terms of the wave excitation (steady loads and low frequency loads) are neglected in the calculation. Indeed, these types of loads induce slowly varying or steady loads in the lines, which are not of interest in this study. Moreover, because of the orientation of the lines (nearly horizontal), we are not expecting VIV loads due to the current.

The mooring lines dynamic analysis is performed using OrcaFlex with a simulation duration set to 1 hour. The same parameters of line discretization, Morison forces parameters as described in part 3 are employed.

The hydrodynamic database composed by radiation, excitation forces and drift forces is calculated using HydroSTAR [15]. Then the wave frequency floating-body motions are computed within OrcaFlex using a coupled analysis with the mooring system. Although no wind forces are considered, the wind turbine assembly has an influence on the mass and inertia of the system. Quadratic viscous damping on the structure is also included in order to achieve realistic vertical motions.

The effective tensions in the front line 1 and rear line starboard side 1 at fairlead and anchor connection points are studied for comparison.

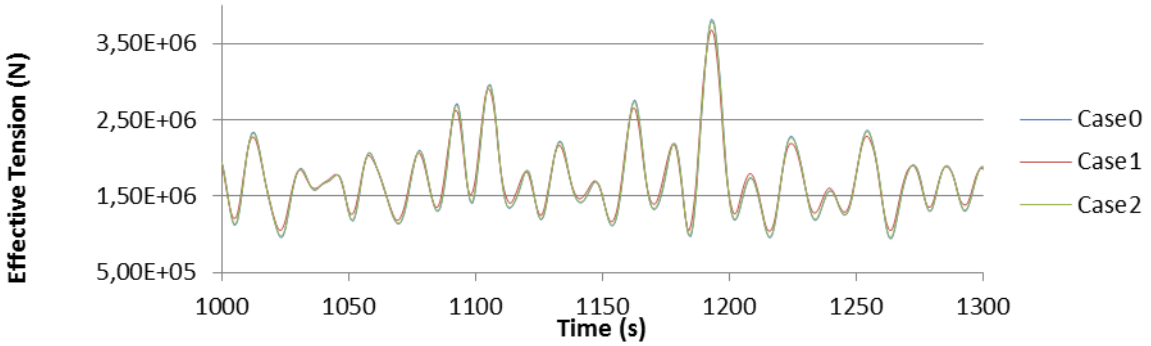

Figure 5.1: Front line 1 tension time history (fairlead), extreme sea state

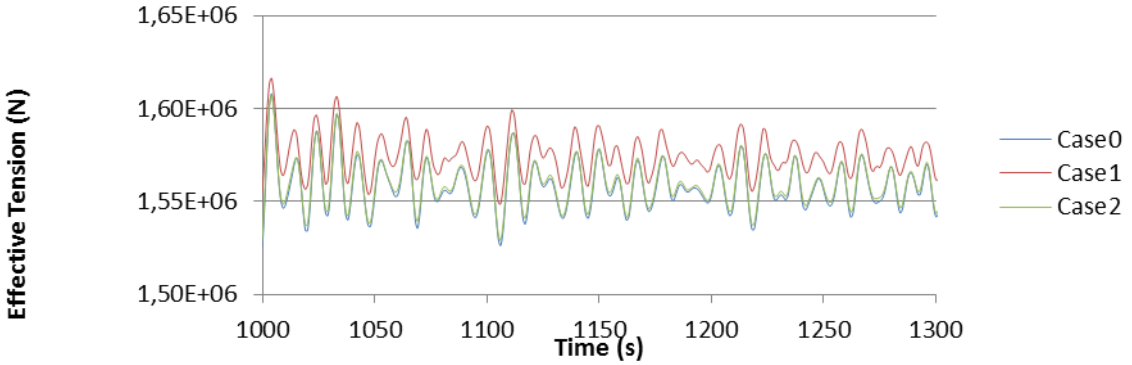

Figure 5.2: Front line 1 tension time history (fairlead), fatigue sea state

Cases 0, 1 and 2 are first compared to assess the effect of the total quantity of marine growth. For the extreme sea state (figure 5.1), it can be seen that there is no significant difference on effective tension time histories (at fairlead points) between all these cases. This is due to the fact that in extreme sea condition, the impact of marine growth on the tension in the taut mooring lines is very small compared to the wave load. However, it should be emphasized that the minimum tension increases with the amount of marine growth present on the line while the maximum tension decreases (table 5.2 and figure 5.3). It is thus observed that the addition of marine growth produces lower maximum tension and tension ranges at the mooring line's fairlead, which is of great benefit to both strength and fatigue design. Similar observations can be made concerning the tension at anchor but the variations are much smaller (table 5.3).

The differences in effective tension time histories are more obvious for the fatigue sea state (figure 5.2). Indeed, the increase in line tension due to the mass of marine growth can be observed. As a result, both maximum and minimum values of effective tension in mooring lines are increasing with the marine growth thickness (tables 5.4, 5.5 and figure 5.4). These variations however are quite negligible. The effect on standard deviations on the other hand is more significant. At the fairlead tension's amplitude are decreased while these are increased at the anchor.

The same conclusions can be made for rear lines with the additional observation that the increase in minimum tension for the extreme sea state is very significant as the tension gets very low.

Variations between uniform (cases 2 and 3) and non-uniform distributions (cases 2.1, 3.1 and 3.2) can be of the same order of magnitude as the variations due to the total

amount of bio mass (ie. from case 0 to cases 2 or 3). No clear trend can be drawn though as both extreme values and standard deviations can be either amplified or reduced.

Table 5.2: Max, min, mean, standard deviation of effective tension at fairlead, sea state 1

	Line Front 1			Line Rear starboard 1		
Tension	case0	case1	case2	case0	case1	case2
Max	3.81E+06	3.67E+06	3.78E+06	2.53E+06	2.51E+06	2.52E+06
Mean	1.66E+06	1.68E+06	1.67E+06	1.55E+06	1.66E+06	1.65E+06
Min	8.32E+05	9.00E+05	8.46E+05	4.01E+03	4.74E+04	9.38E+03
Std	3.59E+05	3.27E+05	3.52E+05	1.47E+04	1.39E+04	1.45E+04

Table 5.3: Max, min, mean, standard deviation of effective tension at anchor, sea state 1

	Line Front 1			Line Rear starboard 1		
Tension	case0	case1	case2	case0	case1	case2
Max	3.83E+06	3.81E+06	3.82E+06	2.53E+06	2.53E+06	2.53E+06
Mean	1.66E+06	1.68E+06	1.67E+06	1.55E+06	1.57E+06	1.55E+06
Min	8.16E+05	8.22E+05	8.18E+05	5.76E+02	5.77E+03	9.39E+02
Std	3.65E+05	3.65E+05	3.65E+05	4.00E+05	3.89E+05	3.98E+05

Table 5.4: Max, min, mean, standard deviation of effective tension at fairlead, sea state 2

	Line Front 1			Line Rear starboard 1		
Tension	case0	case1	case2	case0	case1	case2
Max	1.61E+06	1.62E+06	1.61E+06	1.69E+06	1.70E+06	1.69E+06
Mean	1.56E+06	1.57E+06	1.56E+06	1.65E+06	1.66E+06	1.65E+06
Min	1.52E+06	1.54E+06	1.52E+06	1.59E+06	1.61E+06	1.59E+06
Std	1.39E+04	1.15E+04	1.32E+04	1.47E+04	1.39E+04	1.45E+04

Table 5.5: Max, min, mean, standard deviation of effective tension at anchor, sea state 2

	Line Front 1			Line Rear starboard 1		
Tension	case0	case1	case2	case0	case1	case2
Max	1.62E+06	1.63E+06	1.62E+06	1.69E+06	1.70E+06	1.69E+06
Mean	1.56E+06	1.57E+06	1.56E+06	1.65E+06	1.66E+06	1.65E+06
Min	1.52E+06	1.52E+06	1.52E+06	1.59E+06	1.60E+06	1.59E+06
Std	1.47E+04	1.66E+04	1.49E+04	1.50E+04	1.53E+04	1.50E+04

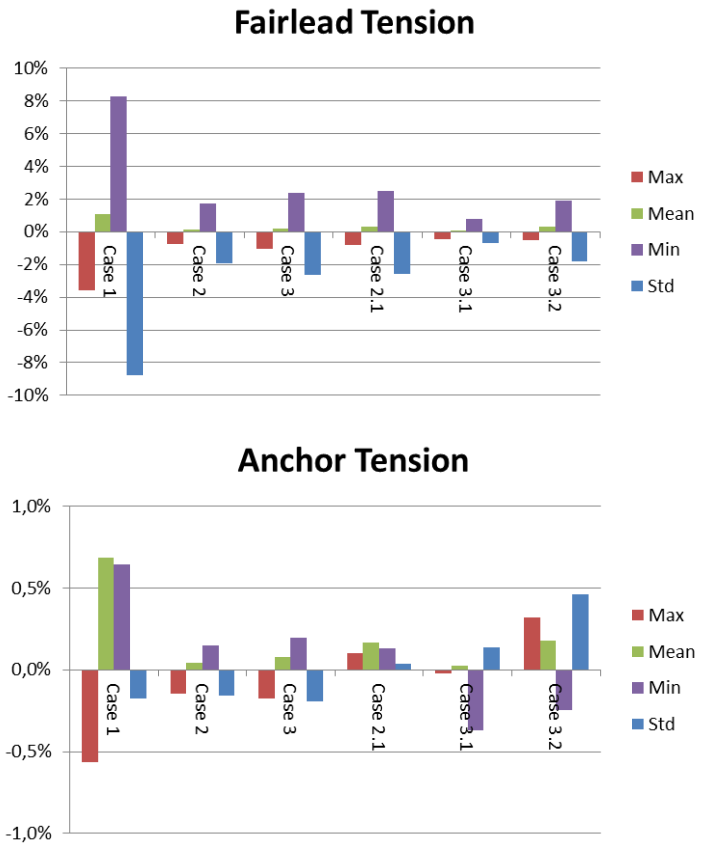

Figure 5.3: Variations from case 0, front line 1, extreme sea state

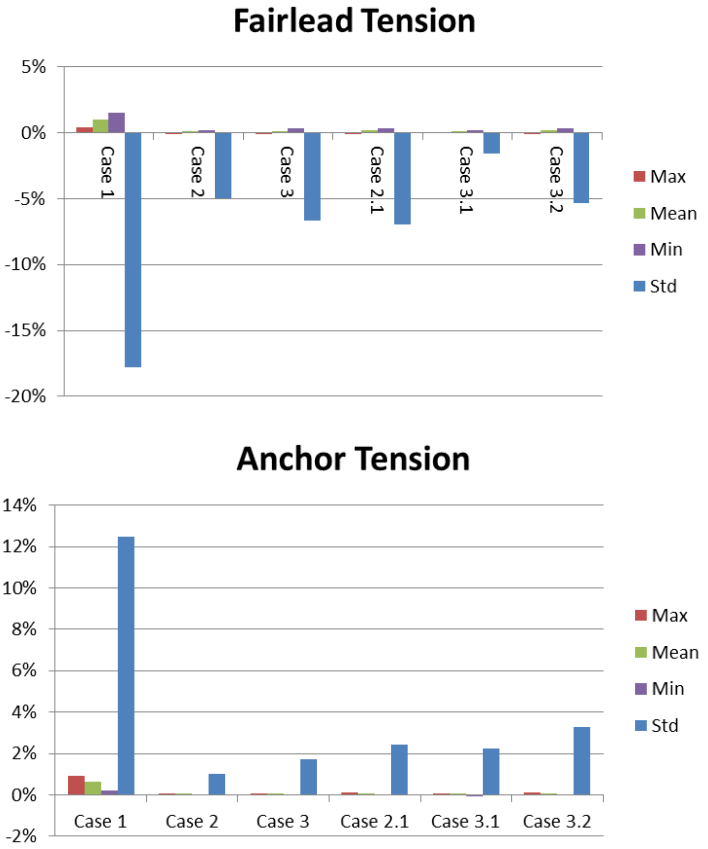

Figure 5.4: Variations from case 0, front line 1, fatigue sea state

Conclusions

Comparisons between in-situ measurements and recommendations from offshore standards about bio-colonization weight and thickness on submerged mooring lines lead to good agreement on maximum thickness. Nonetheless measurements reveal inhomogeneous repartition with reference to vertical position of the line, which could be explained in part by the slippage of the marine species along the line.

When extrapolated to full scale synthetic mooring ropes, the addition of marine growth lead to a large increase of the lineic mass and drag diameter.

The increase in mean tension though is quite negligeable for all the cases studied due to the large pre-tension.

Considering out-of-line axis harmonic excitation, the bio colonization shift the natural frequency toward larger periods at which the floater has a larger response to wave load. The addition of marine growth also tend to increase the dynamic amplification factor due to the increased lineic mass of the line. However this effect remain negligeable when compared to the pre-tension and breaking load of the taut mooring lines.

Tension variations due to in-line excitations are much larger, and though the natural frequencies are higher than the wave frequencies even with bio colonization, some important variations can be observed due to the marine growth. At wave frequencies, tension amplitudes at the fairlead appear to be reduced while increased at the anchor.

When computing the whole system response to irregular sea states, the addition of marine growth on the lines tends to decrease the extremes amplitudes at the fairlead in the extreme sea state. This lead to a lower maximum tension and tension ranges which are benefitial to both strength and fatigue design.

The results obtain with a thiner marine growth layer (2.04 cm), corresponding to the on-site measurements, however exhibit much less variations from the bare line case.

In fatigue sea state, marine growth thickness was shown to be a significant in-line amplification factor of tension amplitudes at the anchor though it reduces amplitudes at the fairlead.

This study, considering nearly horizontal nylon lines in quite shallow water, shows the importance of both the total mass of the biocolinization and the distribution of this mass along the line. In this respect it appears that, considering the on-site measurements, applying a uniform 10 cm thick marine growth layer lead to an over estimation of the effects of the bio colonization. This though seems necessary to account for the possible effects of the non-uniform distribution.

References

[1] H. Mouslim, et al. "Development of the french wave energy test site SEM-REV." *Proceedings of the 8th European wave and tidal energy conference, Uppsala, Sweden*, 2009.

[2] C. Berhault, et al. "SEM-REV, de 2007 à 2016, du projet au site opérationnel: retour d'expérience." *14èmes Journées Nationales Génie Côtier – Génie Civil, Toulon*, 2016

[3] Y. Shun-Han, et al. "The Influence of biofouling on power capture and the fatigue life of mooring lines and power cables used in wave energy converters." *Proceedings of Renew 2016, 2nd International Conference on Renewable Energies Offshore, Lisbon, Portugal,* 2016.

[4] C. Wright, et al. "The dynamic effects of marine growth on a tension moored floating wind turbine." *Proceedings of Renew 2016, 2nd International Conference on Renewable Energies Offshore, Lisbon, Portugal,* 2016.

[5] DNV, GL. "DNV-RP-C205: Environmental conditions and environmental loads." *DNV GL, Oslo, Norway*, 2014

[6] A.P.I. " RP2A-WSD Recommended practice for planning, designing and constructing fixed offshore platforms–working stress design–.", 2000.

[7] NORSOK. "N-003 Actions and action effects 2nd Edition", 2007

[8] Mallat, Chadi, et al. "Marine growth on North Sea fixed steel platforms: insights from the decommissioning industry." *ASME 2014 33rd International Conference on Ocean, Offshore and Arctic Engineering*. American Society of Mechanical Engineers, 2014

[9] Macleod, Adrian K., et al. "Biofouling community composition across a range of environmental conditions and geographical locations suitable for floating marine renewable energy generation." *Biofouling* 32.3 (2016): 261-276.

[10] B. Molin. *Hydrodynamique des structures offshore*. Editions Technip, 2002

[11] H. Ameryoun, F. Schoefs. "Probabilistic Modeling of Roughness Effects Caused by Bio-Colonization on Hydrodynamic Coefficients: A Sensitivity Study for Jacket-Platforms in Gulf of Guinea." *ASME 2013 32nd International Conference on Ocean*, *Offshore and Arctic Engineering*. American Society of Mechanical Engineers, 2013.

[12] T. Sarpkaya. "In-Line And Transverse Forces, On Cylinders In Oscillatory Flow At High Reynolds Numbers." *Offshore Technology Conference*. Offshore Technology Conference, 1976.

[13] Orcina, "User Manual Online at http://www.orcina.com/SoftwareProducts/OrcaFlex/Documentation." , 2012

[14] I. Le Crom, et al. "Extreme sea conditions in shallow water: estimations based on in-situ measurements." *ASME 2013 32nd International Conference on Ocean, Offshore and Arctic Engineering*. American Society of Mechanical Engineers, 2013.

[15] Research department of Bureau Veritas, "HydroStar for expert user manual", June 2016.